

Friction and Adsorption Properties of Normal and High-Oleic Soybean Oils

G. Biresaw^{a,*}, A. Adhvaryu^c, S.Z. Erhan^b, and C.J. Carriere^a

^aBiomaterials Processing and ^bOil Chemical Research Units, NCAUR, ARS, USDA, Peoria, Illinois 61604, and

^cDepartment of Chemical Engineering, Pennsylvania State University, University Park, Pennsylvania 16802

ABSTRACT: The steel/steel boundary friction properties of soybean oil (SBO) and high-oleic soybean oil (HOSBO) are compared. HOSBO is significantly more saturated than SBO and more oxidatively stable. Changes in degree of unsaturation affect lateral interactions of adsorbate molecules, which in turn affects their adsorption and, hence, their boundary lubrication properties. To investigate this possibility, the free energies of adsorption (ΔG_{ads}) of SBO, HOSBO, and methyl laurate (ML) were determined from the analysis of friction-derived adsorption isotherms using the Langmuir and Temkin adsorption models. The results showed a stronger adsorption for the vegetable oils than for ML, an indication of multiple interactions between the ester groups of the triglycerides and the steel surface. The result also showed no difference in the ΔG_{ads} values of SBO and HOSBO obtained using either the Langmuir or Temkin models. This was interpreted as an indication of the lack of appreciable net lateral interaction between triglyceride adsorbates.

Paper no. J9858 in *JAACS* 79, 53–58 (January 2002).

KEY WORDS: Adsorption, adsorption isotherm, boundary additive, boundary lubrication, coefficient of friction, free energy of adsorption, high-oleic soybean oil, methyl laurate, soybean oil, vegetable oil.

Vegetable oils are commercially important products obtained from agricultural sources (1,2). It is estimated that over 16 billion pounds of vegetable oils are produced annually in the United States, of which nearly 80% is soybean oil (SBO) (3). Most vegetable oils are triglycerides (triesters) while some are monoesters of various fatty acid residues. The exact fatty acid composition depends on the source (1,2).

Because of their abundance and because they are renewable source (1–3), vegetable oils are potential substitutes for limited petroleum-based lubricants. Furthermore, vegetable oils are biodegradable, making them very attractive lubricants for use in processes that generate large quantities of liquid and solid effluents, which must be properly treated prior to disposal (4,5).

Vegetable oils can be used in lubricant formulations both as additives and as base oils. Most vegetable oils are liquids at room temperature and are also good solvents for a variety

of substances used in lubricant formulations, thus making them good candidates for use as base oils. At the same time, the ester functionalities along with the long hydrocarbon chains of the fatty acid residues provide vegetable oils with amphiphilic properties, allowing them to be used as boundary additives. Amphiphilic properties affect the boundary lubrication or additive properties while fluid or rheological properties affect the hydrodynamic properties of vegetable oils. Together, these two properties affect the performance of vegetable oils in lubricant applications that occur in boundary, hydrodynamic, and mixed film lubrication regimes.

However, broad application of vegetable oils in lubrication requires solving several problems. The ease of biodegradability of vegetable oils also makes them very susceptible to oxidation or other tribochemical degrading processes that occur under the severe lubrication conditions of high temperature, high pressure, shear, and ambient atmosphere. Various methods are being pursued to reduce or minimize these disadvantages, including the incorporation of various types of inhibitors in the lubricant formulations (6,7). Another approach has been the development of new crops that will provide vegetable oils that are less susceptible to oxidation and other undesirable tribochemical reactions. One result of the latter approach has been the development of high-oleic soybean oil (HOSBO), which has a greater concentration of oleic acid residues than normal SBO (8). Analysis has shown the ratio of oleic to linoleic acid residues of 21:66 and 84:4 for SBO and HOSBO, respectively (Adhvaryu, A., unpublished data). Since oleic acid is a monounsaturate whereas linoleic is diunsaturate, a reduced tendency of oxidation of HOSBO relative to SBO would be expected. Recent studies have confirmed this difference in oxidation properties (7,9).

While reduced unsaturation provides improved oxidation stability, it is not known how it affects the boundary and hydrodynamic lubrication properties of HOSBO relative to SBO. During boundary lubrication, the polar end of the amphiphile adsorbs onto the rubbing surfaces and reduces friction. The degree of friction reduction is highly dependent on the free energy of adsorption (ΔG_{ads}) of the additive onto the surfaces (10,11). When amphiphiles adsorb on surfaces, two types of interactions occur. The primary or adhesive interaction is between the polar groups of the amphiphiles and the surface and is very sensitive to the type and number of functional groups. The lateral interaction is due to dipole-dipole

*To whom correspondence should be addressed at Biomaterials Processing Research Unit, NCAUR, ARS, USDA, 1815 N. University St., Peoria, IL 61604.

E-mail: biresawg@mail.ncaur.usda.gov

and dispersive interactions between adsorbed molecules and is sensitive to such properties as chain length, degree, and stereochemistry of unsaturation (10,11). The ΔG_{ads} is the net interaction energy due to both adhesive and lateral interactions and is obtained by analyzing the adsorption isotherm of an amphiphile on a surface using an appropriate adsorption model. An adsorption isotherm relates the concentration of the amphiphile in solution to that on the surface at constant temperature. Adsorption models that have been used to estimate the ΔG_{ads} of lubricant additives are the Langmuir (12) and the Temkin models (13). The Langmuir model ignores lateral interactions while the Temkin model assumes repulsive lateral interactions.

The objective of this work is to investigate the effect of fatty acid residue chemistry on ΔG_{ads} of SBO and HOSBO on steel surfaces. To accomplish this, the adsorption isotherm of SBO and HOSBO was first determined using boundary friction measurements following the method of Jahanmir and Beltzer (10). Next, the adsorption isotherms were analyzed using both the Langmuir and Temkin adsorption models. The analysis showed no difference in the ΔG_{ads} values of SBO and HOSBO obtained by either model. This was interpreted as an indication of the lack of appreciable net lateral interaction in either oil.

The Jahanmir/Beltzer friction-based adsorption isotherm has been used to measure the ΔG_{ads} for a number of adsorbate/substrate systems (10,11). However, it should be pointed out that application of this method requires that the system being studied meet certain requirements including: (i) adsorption must occur *via* reversible equilibrium for the duration of the friction test, and (ii) friction reduction must be due to the adsorption of the chemicals being studied but not to any tribochemicals generated during the test.

MATERIALS AND METHODS

Lubricants. All lubricant ingredients were obtained commercially and used as supplied. Ingredients used as additives were: normal SBO (Pioneer Hi-Bred International Inc., Des Moines, IA), HOSBO (Optimum Quality Grains, Urbandale, IA), methyl laurate (ML) (99+%; Sigma, St. Louis, MO), and hexadecane (99+% anhyd.; Aldrich Chemical Company, Milwaukee, WI). The lubricant formulations contained 0.003 to 0.6 M of each oil in hexadecane.

Friction measurement. Friction was measured under point contact conditions using a ball-on-disc configuration (Fig. 1) on a Falex[®] Friction & Wear Test Machine, Model Multi-Specimen (Falex Corporation, Sugar Grove, IL). In this configuration, a ball, in contact with a stationary disc, moves around the disc at a specified speed. The resistance to the motion of the ball, i.e., the friction force, is measured by a load cell connected to the disc. The coefficient of friction (COF) is obtained by dividing the friction force by the normal force pressing the ball against the disc. The balls and discs used were obtained commercially (Falex Corporation), then thoroughly degreased by consecutive sonications in fresh reagent-

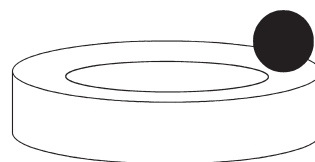


FIG. 1. Schematics of ball-on-disc friction measurement configuration.

grade isopropyl alcohol and hexane (Aldrich Chemical Company) prior to use. The specifications of the balls were: 52100 steel; 12.7 mm (0.5 in.) diameter; 64–66 Rc hardness; extreme polish. The specifications of the discs were: 1018 steel; 25.4 mm (1 in.) o.d.; 15–25 Rc hardness; 0.36–0.46 μm (14–18 $\mu\text{in.}$) roughness. The instrument is equipped with a personal computer and software that allow for automatic acquisition and display of the following set of data at a rate of 1 per second: torque on the disc (friction force), vertical height change (wear), load, speed, lubricant temperature, and specimen temperature. During the test, the COF was automatically calculated and displayed in real time. Data were also saved on a disc for further analysis.

Friction measurement procedure. The ball was fixed on the upper specimen holder for a point contact radius of 11.9 mm (0.468 in.). The disc was fixed on the bottom specimen holder that was enclosed in a cup. Lubricant (50 mL) was poured into the cup so as to completely immerse the ball-on-disc assembly in the lubricant. The disk assembly was then raised and made to contact the ball. The ball was then allowed to rotate and, as soon as it reached the set speed, application of the load began, which was gradually increased until it reached the set value. The friction measurement continued until the set time elapsed. A second test was conducted using the lubricant sample from the first test with a new ball-on-disc specimen. The COF from the duplicate tests were then averaged to obtain the COF of the lubricant being tested. In general, the standard deviation of the COF from the duplicate runs was less than $\pm 5\%$ of their mean.

Friction measurements were conducted at room temperature, for 15 min, at 6.22 mm/s (5 rpm) and 181.44 kg (400 lb) load. The temperature of the specimen and lubricant at the start of the test was $25 \pm 2^\circ\text{C}$. This temperature increased by 1–2 $^\circ\text{C}$ during the 15-min test period.

The COF of pure hexadecane, i.e., lubricant with zero additive concentration, was obtained from the measurement of the COF of hexadecane as a function of load as 45.36–136.08 kg (100 to 350 lb). The COF increased with increasing load until about 113.40 kg (250 lb) after which it leveled off to an average value of 0.50. This COF value of pure hexadecane was later used in the calculation of fractional surface coverages of the additives (see details below).

RESULTS AND DISCUSSION

Dependence of COF on run time. A typical plot of run time vs. COF from a 15-min test run is shown in Figure 2. In all cases, the COF increases with time and levels off to a steady-

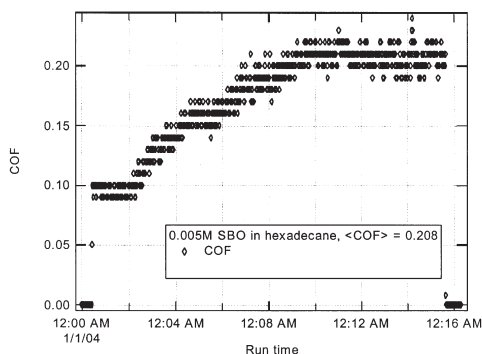


FIG. 2. Run time vs. coefficient of friction (COF) plot of a typical ball-on-disc test. SBO, soybean oil.

state value. The COF value for a particular run is the average COF in the steady-state region. The COF due to a lubricant is the average of the COF from duplicate runs with the same lubricant on separate sets of ball-on-disc specimens. The lubricant COF is used in subsequent data analysis.

Dependence of COF on additive concentration. In Figure 3 the effect of concentration on the COF of SBO, HOSBO, and ML is illustrated. Changes in additive concentrations led to similar trends in COF for all three additives. At low additive concentrations, the COF was very high and close to the value

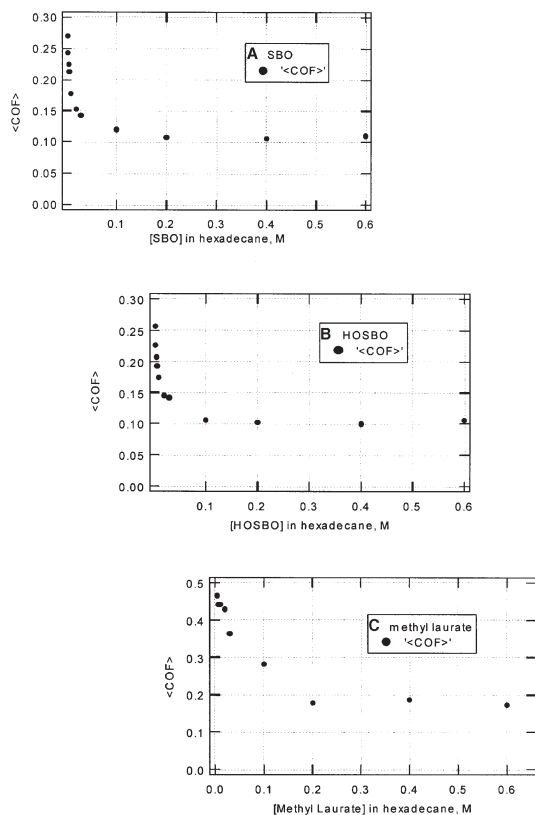


FIG. 3. Effect of additive concentration in hexadecane on mean COF: (A) SBO; (B), high-oleic soybean oil (HOSBO); (C) methyl laurate. See Figure 2 for abbreviations.

of pure hexadecane. As the concentration of additive increased, the COF decreased sharply until it reached a minimum (COF_{\min}) value. The COF value remained constant at COF_{\min} upon further increase in the concentration of additive.

Figure 3 shows the following qualitative differences between the vegetable oils (SBO, HOSBO), which are triesters, and ML, which is a monoester: (i) The rate of decrease of COF with increasing additive concentration was higher for the vegetable oils than for ML; (ii) the minimum additive concentration at which COF_{\min} was observed was lower for the vegetable oils than for ML; and (iii) the value of COF_{\min} was lower for the vegetable oils than for ML. These differences are a direct result of the differences in the chemistry of the additives and will be discussed in subsequent sections.

Friction-derived adsorption isotherm. An adsorption isotherm shows the relationship between the concentration of an additive in base oil and its concentration on the rubbing surfaces. The exact relationship between these two concentrations depends on the adsorption model being considered. Analysis of adsorption isotherms using appropriate adsorption models yields ΔG_{ads} values of the additives on the rubbing surfaces. Such analysis also provides insight into additive/friction surface and additive/additive interactions.

There are various methods of obtaining adsorption isotherms (14). In this work, adsorption isotherms were obtained from boundary friction measurements following the method of Jahanmir and Beltzer (10). In friction-derived adsorption isotherms, the surface concentration of the additive is expressed in terms of fractional surface coverage, θ , which is calculated from boundary COF data as follows:

$$\theta = \theta_a = (f_b - f) / (f_b - f_a) \quad [1]$$

where f_a is COF at full additive coverage or COF_{\min} , f_b is COF of pure base oil, and f is the COF at additive concentrations between 0 and full surface coverage.

In Equation 1, f_a and f_b are constants and are determined experimentally. The value of θ varies between 0 and 1. Its value is 0 at no surface coverage, i.e., $f = f_b$ in Equation 1; and $\theta = 1$ at full surface coverage, i.e., $f = f_a$ in Equation 1. Details of the derivation of Equation 1 are given elsewhere (10).

Estimation of ΔG_{ads} . ΔG_{ads} is the sum of the free energies due to adhesive or primary interaction between the additive and the surface, ΔG_o , and lateral interaction between additive molecules:

$$\Delta G_{\text{ads}} = \Delta G_o + \alpha\theta \quad [2]$$

where α is the net free energy of lateral interaction of additives, and θ is defined above.

Several lateral interactions are summed up to estimate α . Most lateral interactions, including dispersive interactions between hydrocarbon chains, are weakly attractive. However, dipole-dipole lateral interactions are stronger and can be attractive or repulsive. Thus, the net effect of lateral interactions can be attractive ($\alpha < 0$), repulsive ($\alpha > 0$), or incon-

quential ($\alpha \cong 0$). Calculation of ΔG_{ads} using Equation 2 requires values for ΔG_o and α . These values are obtained from the analysis of the adsorption isotherm data using an appropriate adsorption model. In this work, the Langmuir (12) and Temkin (13) adsorption models are used to analyze the friction-derived adsorption isotherm data.

The Langmuir model predicts the following relationship between fractional surface coverage, θ , and solute concentration:

$$\theta = (K_o C)/(1 + K_o C) \quad [3]$$

where C is solute concentration, mol/L. K_o was obtained from the slope of $1/\theta$ vs. $1/C$ plot and used to calculate ΔG_{ads} using Equation 4,

$$\Delta G_{\text{ads}} = \Delta G_o = RT \ln(K_o) \quad [4]$$

where K_o is the equilibrium constant for the displacement of a solvent molecule from the surface by a solute molecule in solution, R is the gas constant, and T is temperature (K).

Equation 4 is similar to Equation 2 at $\alpha = 0$. This is due to the fact that the Langmuir model completely ignores lateral interactions.

In the Temkin model (13), a net repulsive lateral interaction is assumed, i.e., $\alpha > 0$. Thus, Equation 2 is used to calculate ΔG_{ads} using ΔG_o and α values obtained from a Temkin model. The exact equation of the Temkin model used for estimating ΔG_o and α depends on the range of fractional surface coverage being considered (10,11,15–18). For $0.2 \leq \theta \leq 0.8$, the Temkin model reduces to:

$$\theta = (RT/\alpha) \ln(C/K_o) \quad [5]$$

And for $0.8 \leq \theta \leq 1.0$, the Temkin model reduces to:

$$\theta = 1 - (aK_o)(1/C) \quad [6]$$

where $a = (RT/\alpha) [\exp(\alpha/RT)] - 1$.

Equation 5 predicts a linear relationship between θ and $\ln(C)$, whereas Equation 6 predicts a linear relationship between θ and $(1/C)$. In determining ΔG_{ads} using the Temkin model, first the values of α and K_o were obtained from the slope and intercept of $\ln(C)$ vs. θ plot of Equation 5. Then ΔG_o was obtained using Equation 7:

$$\Delta G_o = RT \ln(K_o) \quad [7]$$

Finally, ΔG_{ads} was obtained from Equation 2 at $\theta = 1$, i.e.,

$$\Delta G_{\text{ads}} = \Delta G_o + \alpha \theta = \Delta G_o + \alpha \quad [8]$$

Analysis of friction data. From the friction data in Figure 3, the following minimum COF (or f_a in Eq. 1) were obtained for SBO, HOSBO, and ML, respectively: 0.106, 0.100, and 0.173. A value of 0.5 was estimated for the COF of pure hexa-

decane (f_b in Eq. 1). These values of f_a, f_b , and the friction data of Figure 3 were then used in Equation 1 to calculate the fractional surface coverage, θ , of SBO, HOSBO, and ML. The fractional surface coverages and the corresponding additive concentrations were then analyzed using the Langmuir and Temkin models. From these analyses, the ΔG_{ads} values of SBO, HOSBO, and ML were determined.

The resulting Langmuir isotherms are shown in Figure 4. Plots of $1/[\text{Additive}]$ vs. $1/\theta$ gave good linear fits (correlation coefficients >0.9) for all three additives, with an intercept at 1. From the slopes of these fits, the adsorption equilibrium constant, K_o , was obtained and used to calculate ΔG_o and ΔG_{ads} using Equation 2.

For the Temkin analysis, the $\ln(\text{additive concentration})$ was plotted against the fractional surface coverage, θ . The slope and intercept from the linear fits of the data in the range $0.2 \leq \theta \leq 0.8$ were then used to calculate α and ΔG_o using Equations 5 and 7. These values were then used to calculate ΔG_{ads} using Equation 8. The data plots and linear fits for SBO, HOSBO, and ML used in the Temkin analysis are shown in Figure 5. The linear fits had correlation coefficients of >0.9 .

The ΔG_{ads} results for SBO, HOSBO, and ML calculated using the Langmuir and Temkin models are summarized in

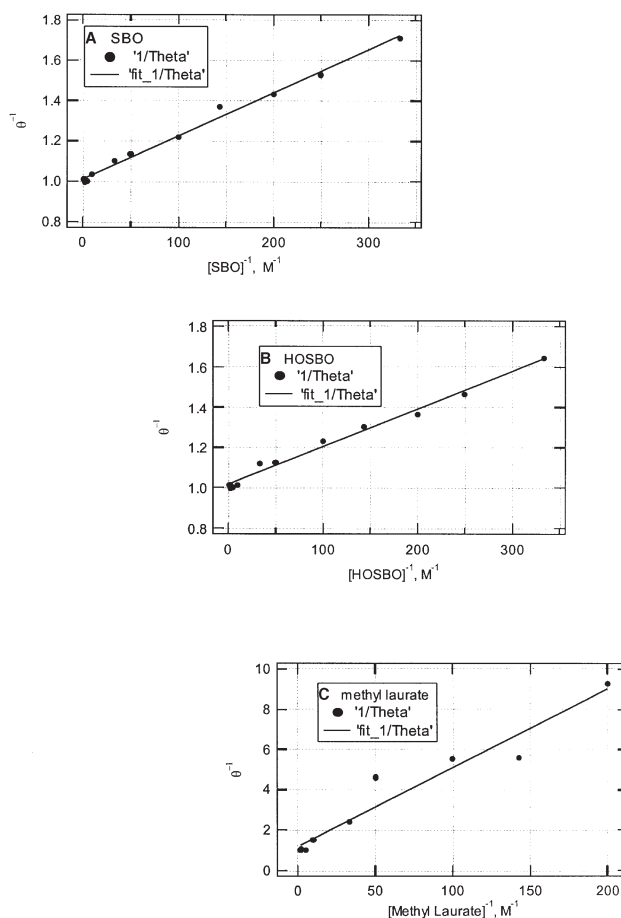


FIG. 4. Langmuir analysis of additive surface coverage (θ) vs. concentration data: (A) SBO; (B) HOSBO; (C) methyl laurate. See Figures 2 and 3 for abbreviations.

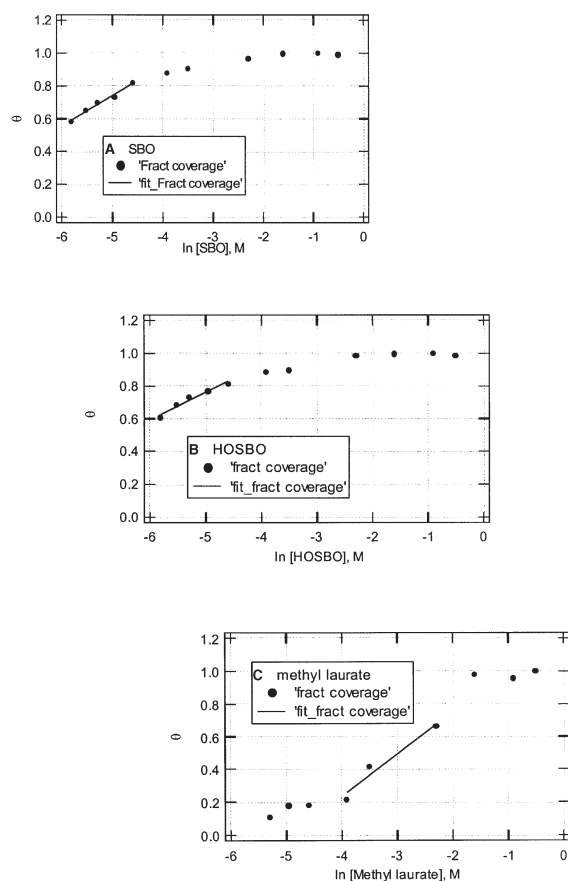


FIG. 5. Temkin analysis of additive surface coverage (θ) vs. concentration data: (A) SBO; (B) HOSBO; (C) methyl laurate. See Figures 2 and 3 for abbreviations.

Table 1. Also included in Table 1 are friction-derived literature ΔG_{ads} data (10,11) of selected monoesters.

Table 1 shows that the vegetable-based soybean and HOSO adsorb more strongly to steel (bigger negative ΔG_{ads} value) than ML. This result is independent of the adsorption model used for calculating the ΔG_{ads} values. This result might

be an indication of more than one ester function of the triester vegetable oil molecule participating in adhesive interaction with the steel surface.

Table 1 shows no difference in the ΔG_{ads} values of SBO and HOSBO obtained using either adsorption model, an indication of similar lubrication properties of SBO and HOSBO in the boundary regime (5,10,11,15–22). This was surprising in view of the large differences in the chain makeup of the two triglycerides and previous reports of strong effects of chain chemistry on ΔG_{ads} (10,11,15–18). The ratio of oleic to linoleic acid residues of SBO and HOSBO are 21:66 and 84:4, respectively. Such overabundances of single unsaturation in SBO and double unsaturation in HOSBO were expected to lead to major differences in lateral interactions, which should show up in a Temkin analysis of the data. The fact that the Temkin analysis showed no such differences might be an indication that lateral interactions canceled each other out, resulting in a net lateral interaction that was too small to interfere with the primary adhesive interaction between the triglycerides and the steel surface. If this is the case, it will be appropriate to analyze the fractional coverage data of triglycerides using the Langmuir rather than the Temkin isotherm. The Langmuir isotherm is derived for systems that do not involve lateral interactions (12) and is also suitable for analyzing systems in which attractive and repulsive lateral interactions cancel out resulting in very small or zero net lateral interaction (10–12,15–18). Additional support for the suggestion that the data from this work are better analyzed using the Langmuir than the Temkin model comes from the comparison of ΔG_{ads} values for ML from this work with the literature (10,11) ΔG_{ads} values of various monoesters (Table 1). It is clear from Table 1 that the literature ΔG_{ads} values of monoesters on steel are much closer to our ΔG_{ads} values from Langmuir analysis than from the Temkin analysis.

ACKNOWLEDGMENTS

The authors wish to thank Haifa Khoury for obtaining the friction data. This work was supported financially by the USDA.

TABLE 1
Friction-Derived Free Energies of Adsorption of Selected Lubricant Additives

Lubricant additive	Friction surfaces	Friction test geometry	Adsorption model	ΔG_{ads} (Kcal/mol)	Reference
Soybean oil	Steel/steel	Ball-on-disc	Langmuir	-3.6	This work
Soybean oil	Steel/steel	Ball-on-disc	Temkin	-2.1	This work
High-oleic soybean oil	Steel/steel	Ball-on-disc	Langmuir	-3.7	This work
High-oleic soybean oil	Steel/steel	Ball-on-disc	Temkin	-2.1	This work
Methyl laurate	Steel/steel	Ball-on-disc	Langmuir	-1.9	This work
Methyl laurate	Steel/steel	Ball-on-disc	Temkin	-0.6	This work
Methyl stearate	Cu/Cu	Ball-on-cylinder	Temkin	-1.3	10
Methyl stearate	Steel/steel	Four-ball	Temkin	-2.5	11
Ethyl stearate	Steel/steel	Four-ball	Temkin	-3.0	11
Methyl oleate	Cu/Cu	Ball-on-cylinder	Temkin	-1.3	10

REFERENCES

1. Salunkhe, D.K., J.K. Chavan, R.N. Adsule, and S.S. Kadam, *World Oil Seed Chemistry, Technology and Utilization*, Van Nostrand Reinhold, New York, 1992, pp. 1–8.
2. Bockish, M. (ed.) *Fats and Oils Handbook*, AOCS Press, Champaign, 1998, 838 pp.
3. Erhan, S.Z., S. Asadauskas, R.O. Dunn, and G. Knothe, Vegetable Oils for Environmentally Friendly Applications, *Proceedings: 48th Oilseed Conference, Competing in World Markets in the New Millennium*, printed by the U.S. Department of Agriculture, Southern Regional Research Center, Agricultural Research Center, New Orleans, 1999, F1–F10.
4. Dick, R.M., Recycling of Metalworking Fluids, *Manuf. Eng. Mater. Process.* 41:339–365 (1994).
5. Schey, J.A., *Tribology in Metalworking Friction, Lubrication and Wear*, American Society of Metals, Metals Park, OH, 1983, pp. 27–130.
6. Becker, R., and A. Knorr, An Evaluation of Antioxidants for Vegetable Oils at Elevated Temperatures, *Lubr. Sci.* 8:95–117 (1996).
7. Asadauskas, S., J.M. Perez, and J.L. Duda, Oxidative Stability and Antiwear Properties of High-Oleic Vegetable Oils, *Lubr. Eng.* 52:877–882 (1996).
8. Haumann, B.F., Modified Oil May Be Key to Sunflower's Future, *inform* 5:1210 (1994).
9. Adhvaryu, A., S.Z. Erhan, Z.S. Liu, and J.M. Perez, Oxidation Kinetics of Oils Derived from Unmodified and Genetically Modified Vegetables Using PDSC and NMR Spectroscopy, *Thermochim. Acta* 364:87–97 (2000).
10. Jahanmir, S., and M. Beltzer, An Adsorption Model for Friction in Boundary Lubrication, *ASLE Trans.* 29:423–430 (1986).
11. Jahanmir, S., and M. Beltzer, Effect of Additive Molecular Structure on Friction Coefficient and Adsorption, *J. Tribol.* 108:109–116 (1986).
12. Langmuir, I., The Adsorption of Gases on Plane Surfaces of Glass, Mica, and Platinum, *J. Am. Chem. Soc.* 40:1361–1402 (1918).
13. Temkin, M.I., Adsorption Equilibrium and the Kinetics of Processes on Nonhomogeneous Surfaces and in the Interaction Between Adsorbed Molecules, *J. Phys. Chem. (USSR)* 15:296–332 (1941).
14. *Principles of Colloid and Surface Chemistry*, 2nd edn., P.C. Hiemenz, Marcel Dekker, New York, 1986, 815 pp.
15. Jahanmir, S., Chain Length Effects in Boundary Lubrication, *Wear* 102:331–349 (1985).
16. Beltzer, M., and S. Jahanmir, Role of Dispersion Interactions Between Hydrocarbon Chains in Boundary Lubrication, *ASLE Trans.* 30:47–54 (1987).
17. Beltzer, M., and S. Jahanmir, Effect of Additive Molecular Structure on Friction, *Lubr. Sci.* 1:3–26 (1988).
18. Beltzer, M., Assessing Adsorption of Conventional Friction Modifying Molecules by Relative Contact Potential Difference Measurements, *J. Tribol.* 114:675–682 (1992).
19. Lockwood, F.E., and K. Bridger, Liquid Wetting on Metal Surfaces and the Heat of Immersion/Adsorption in Lubrication, *ASLE Trans.* 30:339–354 (1987).
20. Lockwood, F.E., K. Bridger, and S.M. Hsu, Heats of Immersion, Friction, and Wear of Base Oil Fractions, *Tribol. Trans.* 32:506–516 (1989).
21. Benchaita, M.T., S. Gonsel, and F.E. Lockwood, Wear Behavior of Base Oil Fractions and Their Mixtures, *Ibid.* 33:371–383 (1990).
22. Benchaita, M.T., R.D. Schwartz, and F.E. Lockwood, Separation and Tribological Evaluation of Paraffinic Base Stocks, *Ibid.* 33:85–95 (1990).

[Received January 2, 2001; accepted October 24, 2001]